SERI/TP-631-664

CONF-801102--24



# ANALYSIS OF THE MIST LIFT PROCESS FOR MIST FLOW OPEN-CYCLE OTEC

ROGER L. DAVENPORT

JUNE 1980

TO BE PRESENTED AT
THE 1980 ASME WINTER
ANNUAL MEETING
CHICAGO, ILL., 16-21 NOV. 1980

PREPARED UNDER TASK NO. 3451.20

**Solar Energy Research Institute**
A Division of Midwest Research Institute

1617 Cole Boulevard
Golden, Colorado 80401

Prepared for the
U.S. Department of Energy
Contract No. EG-77-C-01-4042

## DISCLAIMER

Printed in the United States of America
Available from:
National Technical Information Service
U.S. Department of Commerce
5285 Port Royal Road
Springfield, VA 22161
Price:
Microfiche $3.00
Printed Copy $ 4.00

# Analysis of the Mist Lift Process for Mist Flow Open-Cycle OTEC

by

Roger L. Davenport
Associate Engineer
Solar Energy Research Institute
1617 Cole Blvd.
Golden, Colo. 80401

ABSTRACT

Preliminary results are presented of a numerical analysis to study the open-cycle mist flow process for ocean thermal energy conversion (OTEC). Emphasis in the analysis is on the mass transfer and fluid mechanics of the steady-state mist flow. The analysis is based on two one-dimensional models of the mist lift process: a single-group model describes a mist composed of a single size of drops and a multigroup model considers a spectrum of drop sizes. The single-group model predicts that the lift achieved in the mist lift process will be sensitive to the inlet parameters. Under conditions that lead to maximum lift in the model for a single drop size, the multigroup model predicts significantly reduced performance. Because the growth of drops is important, sensitivity of the predicted performance of the mist lift to variations in the collision parameters has been studied.

NOMENCLATURE

| | |
|---|---|
| $a_{ij}$ | geometrical collision cross-section between groups i and j ($m^2$) |
| A | area of cross-section of lift tube ($m^2$) |
| $A_o$ | total area of orifices ($m^2$) |
| $C_d$ | drag coefficient |
| $C_p$ | specific heat of water (J/kg-K) |
| d | drop diameter (m) |
| D | diameter of lift tube (m) |
| $f_{ij}$ | rate of collisions between groups i and j per unit volume ($1/m^3$-s) |
| $F_{ij}$ | rate of coalescences between groups i and j per unit length (1/m-s) |
| g | acceleration due to gravity ($m/s^2$) |
| $G_i$ | total number of drops lost from group i due to coalescence with other drops per unit length (1/m-s) |
| $h_{fg}$ | latent heat of vaporization of water (J/kg) |
| h | specific enthalpy (J/kg) |
| m | mass of drop (kg) |
| n | number flux of drops (in a unit mass interval) (1/s) |
| p | pressure (bar) |
| $S_i$ | source of drops in group i per unit length (1/m-s) |
| t | time (s) |
| T | temperature (K) |
| v | velocity (m/s) |
| w | mass flow rate (kg/s) |
| z | vertical coordinate (m) |
| $\eta$ | coalescence efficiency |
| $\mu$ | viscosity (N-s/$m^2$) |
| $\rho$ | density ($kg/m^3$) |
| $\sigma$ | surface tension ($N/m^2$) |

Subscripts

| | |
|---|---|
| f | liquid |
| g | vapor |
| i | individual group of drops in multigroup model |
| j | jet |
| o | stagnation (before orifices) |
| l | bottom of lift tube (after orifices) |

INTRODUCTION

The mist flow concept is a promising alternative to closed-cycle and other open-cycle ocean thermal energy conversion (OTEC) concepts (1). This concept eliminates the heat exchanger losses of the closed cycle and the huge turbines of the steam-based open cycle in favor of a single direct-contact condenser and a standard hydraulic turbine. The mist lift tube, the major component of a mist flow OTEC plant, converts the thermal energy of surface seawater into gravitational potential energy, which is transformed into useful work by the hydraulic turbine. Figure 1 shows a possible configuration for a mist flow power plant, with the hydraulic turbine located upstream of the mist lift tube. Useful power is obtained from the generator connected to the turbine.

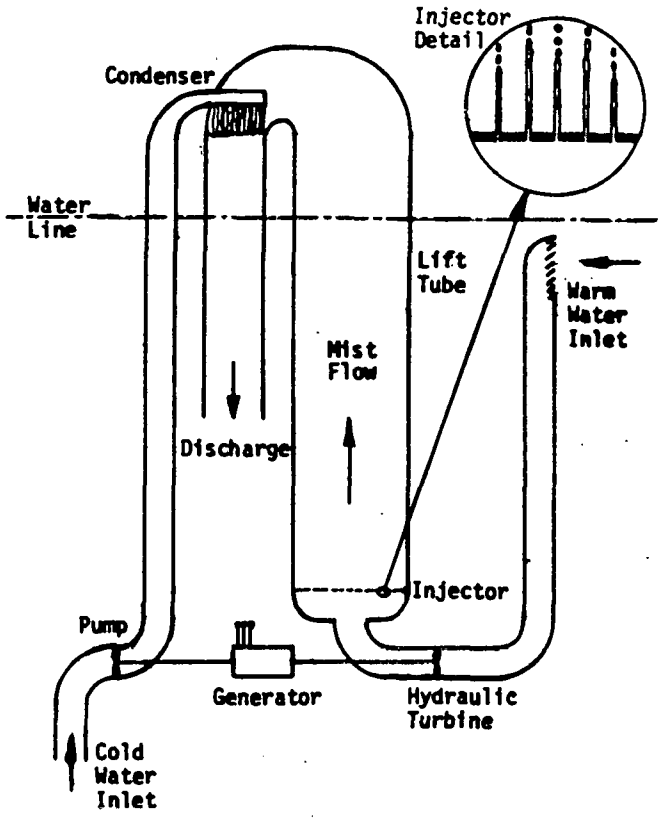


Figure 1. Schematic of Mist Flow Power Plant

The lifting of the water against gravity inside the lift tube is accomplished by the vertical flow of a mist of water droplets entrained in low-pressure water vapor. To produce the mist, the warm water is injected into the bottom of the evacuated lift tube in small jets which break up into drops of a few hundred microns in diameter by Rayleigh instability. The pressure in the lift tube is maintained at a value less than the saturation vapor pressure of the warm water so the drops evaporate. The vapor produced by the evaporating drops expands upward, carrying the water drops along by viscous drag to the top of the lift tube, where cold water from the ocean depths is used to condense the vapor and the liquid drops are collected.

Although the thermodynamics of the mist lift process are relatively straightforward and support its viability, the fluid mechanics of the flow are not well understood. Major areas of concern are the creation of the mist and the possibility of droplet growth leading to "rainout," where the drops are no longer able to be supported by the vapor and fall back down the tube like rain. An understanding of the fluid mechanics of the mist lift process is necessary to assess its viability and its sensitivity to variations in the operating parameters. In parallel with the experimental investigations of the mist flow process conducted at the University of California at Los Angeles (2), the Solar Energy Research Institute (SERI) began an analytical investigation in FY79 to delineate the important fluid mechanic parameters of the process (3).

Two models of the mist flow have been developed: one model considers a mist composed of a single size of drops, and the other considers a spectrum of drop sizes so that effects of collisions and growth of the drops are included. The mathematical formulation of the models is detailed in the Appendix.

## DESCRIPTION OF THE SINGLE-GROUP MIST FLOW MODEL

The single-group analysis is steady-state and one-dimensional along the mist tube. No attempt has been made to model three-dimensional effects such as drop deposition on the walls of the tube or large-scale instabilities that might arise. The purpose of this analysis was to indicate the effect of droplet growth on the performance of the mist lift, and it was felt that the additional complication of multi-dimensional effects was not justified at this point. It is expected that such effects may be significant, especially since the flow of vapor is turbulent, and experimental studies need to be performed to determine the magnitude of the effects.

The following procedure is employed for the solution of the governing equations in this model (as detailed in the Appendix). Input parameters are the drop size, the liquid mass flow rate, the pressure upstream of the injector, the total area of injector holes, the inlet temperature, the condenser temperature, and the geometric shape of the lift tube. By using the inlet parameters in Bernoulli's equation, the equilibrium pressure just inside the lift tube is calculated, which determines the equilibrium temperature and amount of temperature flashdown of the warm water. The drops are assumed to form and their flashdown to equilibrium temperature is assumed to occur within the first vertical step. This assumption is reasonable for the drop sizes encountered due to the high thermal diffusivity of the water. Once the inlet conditions are established, a step size up the tube is chosen and the droplet momentum equation is employed to find the change in drop velocity over that step up the tube. A forward finite difference expression is used to approximate the derivative of velocity with respect to height. The overall momentum, mass, and energy conservation equations for the flow are solved simultaneously to yield the changes in steam quality, pressure, and vapor velocity for the step to the new location. Finally, the drop velocity, quality, pressure, and vapor velocity variables are updated for the new location, the change in droplet mass due to evaporation is calculated, and output is generated. This process is repeated until the point is reached where the equilibrium bulk temperature becomes less than the specified condenser temperature, or until the droplet velocity is less than zero. If calculation stops because the bulk temperature reaches the temperature of the condenser, the drops may have considerable kinetic energy remaining. Further lift could be realized in a suitably designed "coasting" section of lift tube. Such a coast section would be designed to recover the kinetic energy of the flow by allowing it to follow a ballistic trajectory without temperature change. The occurrence of negative drop velocities implies "rainout" because the drops are no longer lifted by the vapor and begin to fall back down the lift tube. In either case, the lift height is defined as the height at which one of the above conditions is met.

## DESCRIPTION OF THE MULTIGROUP MIST FLOW MODEL

To study the effects of droplet growth by coalescence, the multigroup model was developed to consider a spectrum of drop sizes (Ref. 4 and appendix). The single-group model discussed in the

preceding section is the degenerate case of this model with one drop size. In the multigroup model, drops are apportioned into a series of discrete sizes, the masses of which are contiguous integral multiples of a chosen base mass. Thus, the mass of a drop in group j is taken to be $(j \cdot m_1)$, where $m_1$ is the mass of each drop in group 1. Fifty drop sizes constitute the spectrum, which gives a range of drop sizes up to about four times the diameter of the drops in the first group. Equal mass intervals between groups were chosen so that drops from groups i and j would coalesce to form a drop in group (i + j).

The multigroup model algorithm is similar to the algorithm for the single-group model described in the preceding section. Instead of one specific drop size, an initial distribution of drops is input. All other inputs are the same as for the single-group model. At the bottom of each step up the lift tube, calculations are made of the interactions among the 50 groups of droplets to determine the evolution of the drop-size spectrum due to collisions. A geometric collision cross-section based on the diameters and speeds of the interacting drops is used, and a coalescence efficiency is calculated based on the diameters of the interacting drops. For each group of drops, the droplet momentum equation is applied to obtain the average velocity of the group. Finally, solution of the overall conservation equations yields the temperature, quality, and vapor velocity at each step. Thus, the flow properties and the evolution in size and velocity of the drop spectrum are obtained as the mist proceeds up the lift tube. The calculation is terminated when the equilibrium temperature becomes the temperature specified for the condenser, or when any group of drops acquires a zero velocity, implying rainout.

The model includes an algorithm to "squish" the spectrum of drop sizes when it becomes full of drops. Conserving mass and momentum, the algorithm combines the groups of drops in the 50-drop spectrum by pairs into the smallest 25 drop sizes of a new 50-drop-size spectrum with a mass increment twice that of the original spectrum. Calculation then proceeds with the new spectrum. The criterion chosen for this process was to squish whenever the number of groups containing more than 1% of the total mass flow exceeded a value of eight. This criterion led to consistent squishing of the spectrum without large losses at the end of the spectrum and without overly limiting its extent.

The coalescence efficiency model was based on the results of Abbott (5) for drops falling in air at their terminal velocities. The probability of coalescence was digitized from Abbott's results for the range of drop sizes encountered in the mist flow and entered as a subroutine to the multigroup mist lift computer program. Pairs of drops not coalescing were assumed to separate without satellite drops or exchange of mass. Also coded into the program was an upper limit on drop size based on the balance of the drop's surface tension and fluid pressures from the flow, so that drops could not combine to create a drop larger than the limiting drop size.

## RESULTS

A plot of the velocities of the largest and smallest drops in the spectrum and the velocity of the vapor from a single run of the multigroup model is given in Fig. 2. The drop-size distribution measured by Charwat (2) for an injector designed for the mist flow was used as the initial drop-size spectrum. The inlet drop-diameter spectrum has a mean of 0.176 mm and a standard deviation of 0.030 mm and is approximately Gaussian in shape. The two downward-sloping curves in Fig. 2 are the velocities of the smallest and largest drops in the spectrum as it develops up the length of the lift tube. The third curve is the plot of vapor velocity versus distance up the tube. The points at which squishing of the spectrum occurred are indicated by the downward-pointing arrows and show growth of the droplets by coalescence is significant. The lift height achieved is only 26.6 m more than the height to which the drops would rise ballistically in the absence of drag, given their inlet velocity.

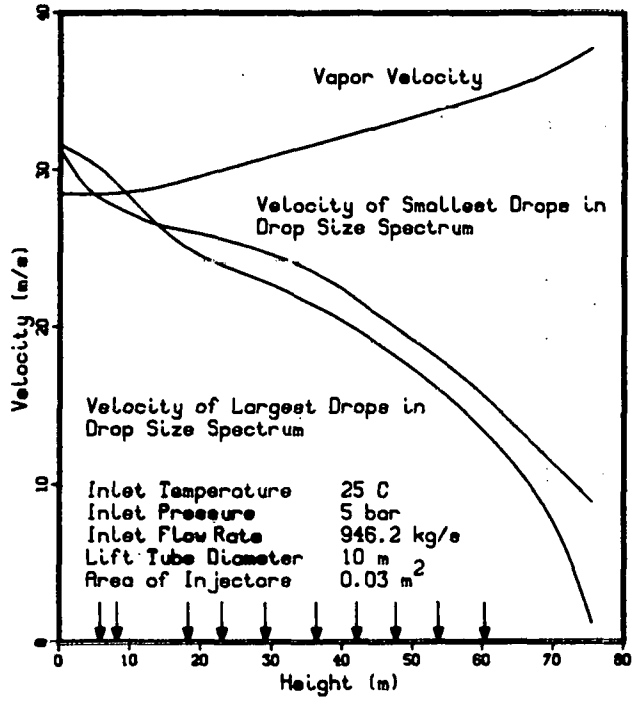


Fig. 2. Velocity predictions of the multigroup mist flow model

The lift height predicted by both models is quite sensitive to the inlet conditions, especially the mass flow rate and pressure upstream of the injector. This sensitivity is evident in Fig. 3, where the results obtained from the two models are plotted as curves of predicted lift height versus mass flow rate at two selected inlet pressures. The range of mass flow rate for each of the two inlet pressures corresponds to the pressure just inside the lift tube varying from the saturation vapor pressure of the inlet warm water to that associated with the temperature of the condenser. Thus, the mass flow rates span from the condition of no flashdown at the entrance of the lift tube to the condition where the inlet warm water flashes down immediately to the condenser temperature. For a given set of conditions, variation of the flow rate by as little as 1% leads to large changes in the predicted lift height (neglecting possible recovery of kinetic energy by a coast phase at constant temperature).

The single-group model results, plotted as solid lines in Fig. 2, are explained as follows. In the low-flow-rate region of the curves, the pressure calculated for the bottom of the lift tube from Bernouilli's equation is relatively high. This means that little flashing of the warm water to steam occurs and thus the vapor velocity is small. The drops are

injected into this almost stagnant vapor and are slowed by drag forces and gravity until they stop, so that rainout occurs after only a few metres. The steep jump at the low-flow-rate side of each of the curves corresponds to the flow rate at which just enough vapor is generated by flashing of the warm water to accelerate the drops up the tube just before they stop due to the force of gravity. This condition leads to a maximum lift height. As the flow rate is increased further, the predicted pressure at the bottom of the lift tube decreases, which leads to increased flashdown of the warm water and higher vapor velocities at the inlet. Since the temperature at the entrance decreases as the flow rate increases, the condenser temperature is reached at a lower height and the model predicts a decreased lift height. However, the velocities of the vapor and droplets are not zero when the temperature of the condenser is reached, and kinetic energy is available for recovery by coasting. The high-flow-rate cutoff of each of the curves corresponds to the flow rate at which the flashdown temperature of the water is calculated to be the temperature of the condenser immediately upon its entrance; the calculation is terminated at that point.

The results of the multigroup model are shown in Fig. 3 as dashed curves. In the multigroup model, the growth of the drops in the spectrum causes the drops to rain out in a short distance unless there is enough flashing of the warm water to generate a substantial amount of vapor to sustain the drops as they grow. The predicted lift for the low-flow-rate portion of each curve, where the flashdown is small, is therefore much less for the multigroup model than for the single-group model. As the flow rate is increased, the amount of flashdown and, hence, the amount of vapor generated increase. Thus, the vapor velocity increases, and the drops are lifted more by the vapor before raining out. This process yields an increasing lift height before rainout with increasing flow rate, as shown in Fig. 3. This increase in predicted lift height with flow rate continues to a point at which the flashdown temperature becomes nearly equal to the condenser temperature. At this point, the multigroup model predicts the greatest lift height. Beyond the point of maximum predicted lift height, the multigroup model results are similar to the single-group model results; the predicted lift decreases because the temperature of the condenser is soon reached. However, the drops still have kinetic energy at that point.

In Fig. 3, the reduction in the maximum lift height predicted by the single-group model for the higher inlet pressure is the result of a combination of increased inlet losses and exit kinetic energy losses at the higher inlet pressure. The multigroup model predicts an increase in maximum lift height at the higher inlet pressure because the injection velocities increase with the inlet pressure, and thus the ballistic height is increased.

To assess the effect of the coalescence efficiency model on the predictions of the multigroup model, the original results were compared with the results obtained with the coalescence efficiency set at unity and at one-half of the value obtained from Abbott. Figure 4 summarizes the results of this parametric study.

With a coalescence efficiency of one (i.e., all collisions resulting in coalescence), the results do not greatly differ from the original results. This is expected for the drops while they are small because the coalescence efficiency is very near unity for drops less than 1 mm in diameter. The slight increase in lift height achieved with a coalescence efficiency of one is due to the formation of larger drops that are not slowed as much by the low-velocity vapor at the entrance.

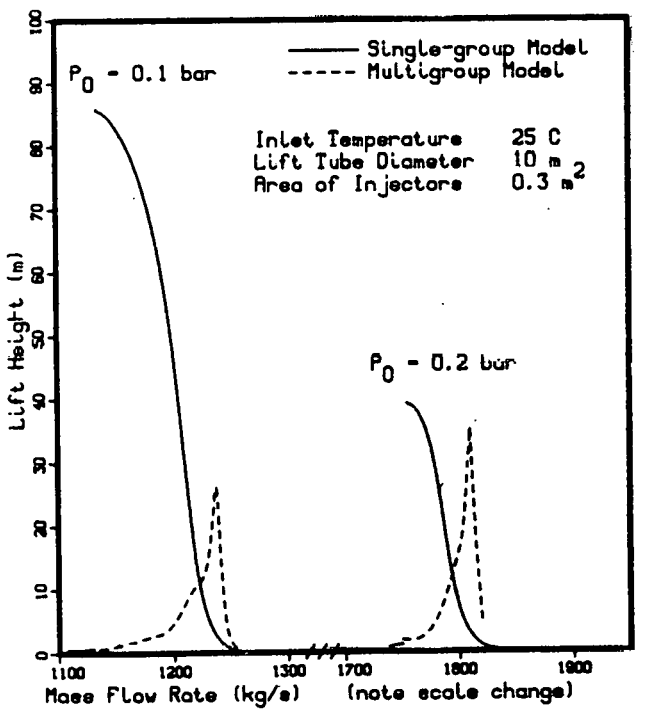


Fig. 3. Comparison of Single-group and Multigroup Results.

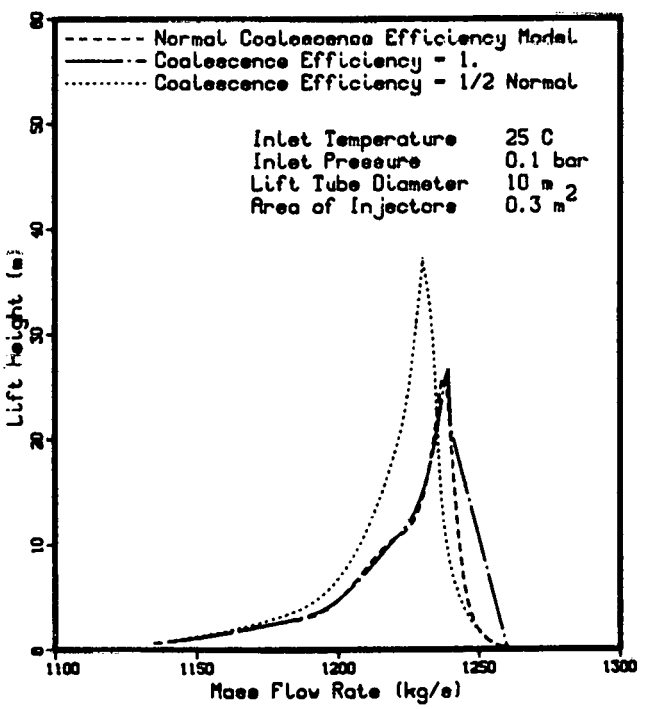


Fig. 4. Lift Height Predicted by Multigroup Model for Various Values of the Coalescence Efficiency.

With a coalescence efficiency of one-half of the value obtained from Abbott's results, the difference in the results is much more pronounced. The reduction in droplet growth causes the drops to be lifted more effectively by the vapor and to rise further before rainout.

## CONCLUSIONS

The most significant conclusion from the single-group model is that the predicted lift produced by the mist flow is strongly dependent on the inlet conditions. Small variations in the mass flow rate at a given inlet pressure, corresponding to small changes in the amount of flashing by the warm water at the inlet, produce large variations in the predicted lift height. Also, the maximum lift is obtained just on the brink of collapse of the mist flow. The current injector design, which causes the drops to be injected into an almost stagnant layer of vapor, results in large friction losses at the entrance of the lift tube and a sharp low-flow-rate cutoff in the allowable pressure/flow rate operational envelope. An injector designed to allow the drops to be introduced at nearly the velocity of the vapor over a wide range of flow rates would alleviate this problem.

The results of the multigroup model indicate that the growth of droplets by collision and coalescence is significant. Compared to the results of the single-group model, the growth of the drops in the mist predicted by the multigroup model reduces the lift height achieved and the range of operation possible without rainout. Maximum lift is achieved when a large amount of flashing of the warm water occurs at the inlet of the lift tube, producing sufficient vapor to lift the drops while they are still small. Sensitivity of the results to the coalescence efficiency model indicates that mechanisms that reduce the coalescence efficiency or produce small drops are important in increasing the lift height achieved by the mist flow. Therefore, efforts are now being made to include the collision-induced breakup of drops, which is expected to reduce the maximum size attained by drops and to produce small drops.

## ACKNOWLEDGMENTS

This work was conducted under contracts, managed by Bill Richards, with the Department of Energy. The original mist flow models described in this paper were developed by Graham Wallis and his associates at the Thayer School of Engineering, Dartmouth College. The assistance and guidance of Dave Johnson and Ben Shelpuk of SERI were invaluable in this task.

## REFERENCES

1. Ridgway, S. L., and Hammond, P. R., "Mist Flow Ocean Thermal Energy Process," RDA-TR-107800-002, Sept. 1978, Research and Development Assoc., Marina del Rey, Calif.

2. Charwat, A. G., "Studies of the Vertical Mist Transport Process for an Ocean Thermal Energy Cycle," SAN/0034-76-1, Nov. 1978, University of California at Los Angeles.

3. Davenport, Roger, "Mist Lift Analysis Summary Report," SERI/TR-631-627, July 1980, Solar Energy Research Institute, Golden, Colo.

4. Wallis, G. B., Richter, H. J., and Bharathan, D., "Analysis of the OTEC Mist Lift Process," SERI-8317-1, 1979, Thayer School of Engineering, Dartmouth College, N.H.

5. Abbott, C. E., "A Survey of Waterdrop Interaction Experiments," Reviews of Geophysics and Space Physics, Vol. 15, Aug. 1977, pp. 363-374.

## APPENDIX[1]

### N-Group Mist Lift Model

The droplets are divided up into groups, and the mass of each group is an integral multiple of the mass of the smallest group, designated by subscript 1. Thus, if group 1 has a diameter of 0.2 mm and a mass of 4.19 μg, then group 2 has a diameter of 0.252 mm and a mass of 8.38 μg, group 3 has a diameter of 0.288 mm and a mass of 12.6 μg, and so on.

The diameter, mass, and velocity of the drops in group 'i' are denoted by $d_i$, $m_i$, and $v_i$, respectively. The overall flow rate of these drops is $n_i$ (number per unit time over the cross-sectional area of the lift tube, A). The number of these drops per unit volume at any location is then $n_i/Av_i$.

Collisions. The rate of collisions between drops from species i and j per unit volume is

$$f_{ij} = \left(\frac{n_i}{Av_i}\right)\left(\frac{n_j}{Av_j}\right)|v_i - v_j|\, a_{ij} \quad , \tag{1}$$

where $a_{ij}$ is a collision cross-section. From a review of the literature and, in particular, the results of Abbott (5), it appears reasonable to assume that the drops move in straight lines and that any geometrical interference between their trajectories leads to either coalescence or separation. Therefore, the collision cross-section is

$$a_{ij} = \frac{\pi}{4}(d_i + d_j)^2 \, . \tag{2}$$

A coalescence efficiency $\eta$ is introduced to account for the finite probability that the result of the collision is the creation of a drop in group $(i + j)$. Drops not coalescing are assumed to split apart, retaining their original identities. The total rate of collisions resulting in coalescence between drops in groups i and j in length dz of the column is obtained from Eqs. (1) and (2):

$$F_{ij}dz = Af_{ij}\eta dz = \frac{n_i n_j}{Av_i v_j}|v_i - v_j|\frac{\pi}{4}(d_i + d_j)^2\eta dz. \tag{3}$$

As long as dz is infinitesimally short there will be no multiple collisions, nor will the number of collisions be limited by the droplet flow rate in a given group. However, these effects must be considered in a finite difference numerical scheme.

The total number of collisions resulting in a loss of drops in group i in a distance dz is

$$G_i = \sum_{j=1}^{k} F_{ij}dz,$$

where k is the number of groups in which there are droplets. There is no need to remove the self-collision term $F_{ii}$; its value is zero because $|v_i - v_i| = 0$. At the same time, drops are created in group i by collisions over all combinations of drops

[1] Adapted from Ref. 4.

in groups j and r for which j + r = i. By letting "r" always represent the heavier drop in a collision, the source of drops in group i per unit length is

$$S_i = \sum_{j=1}^{INT(i/2)} F_{j(i-j)}dz \ , \qquad (4)$$

where INT(i/2) represents the largest integer that is less than or equal to i/2.

The conservation equation for drops in group i is then

$$\frac{dn_i}{dz} = \sum_{j=1}^{INT(i/2)} F_{j(i-j)} - \sum_{j=1}^{k} F_{ij} \ . \qquad (5)$$

Integration of Eq. (5) enables the evolution of the droplet size spectrum to be computed.

Drop Momentum. Consider a control volume which spans the lift tube horizontally and has a height dz. We may formulate a momentum balance on the drops of group i passing through the control volume as follows. The incoming drops in a group i transport momentum at a rate of $(n_i m_i v_i)_z$. The outgoing drops carry away momentum at a rate of $(n_i m_i v_i)_{z+dz}$. The drops added to group i by collisions contribute a momentum equal to

$$\sum_{j=1}^{INT(i/2)} F_{j(i-j)}(m_j v_j + m_{i-j} v_{i-j})dz.$$

The drops that are removed from group i by collisions cause a loss of momentum of

$$(m_i v_i)\sum_{j=1}^{k} F_{ij}dz \ .$$

Evaporation leads to a loss of momentum of $-n_i v_i dm_i$. The important forces on the drops in the control volume are gravity and the drag force on the drops from the steam. The overall momentum balance is then

$$n_i m_i dv_i + m_i v_i dn_i + n_i v_i dm_i$$

$$- \sum_{j=1}^{INT(i/2)} \{F_{j(i-j)} (m_j v_j + m_{i-j} v_{i-j})dz\} + n_i v_i dm_i$$

$$- m_i v_i \sum_{j=1}^{k} \{F_{ij}dz\}$$

$$+ \frac{n_i}{v_i} \left[C_{d,i} \frac{\pi d^2}{8} \rho_g |v_g - v_i|(v_g - v_i) - m_i g\right]dz \ . \qquad (6)$$

The small contribution to the force term from the pressure gradient is neglected. There is also some question about how to handle the interchange of momentum between the phases due to evaporation: Which phase is "charged" for how much of the momentum change $(v_g - v_i)dm_i/dz$? At this stage this is neglected in the momentum equation. In fact, all contributions in Eq. (6) resulting from $dm_i/dz$ are neglected, which reduces Eq. (6) to a differential equation involving $dn_i/dz$ and $dv_i/dz$.

Substituting from Eq. (5), we obtain an explicit equation for $dv_i/dz$:

$$\frac{dv_i}{dz} = \frac{1}{m_i v_i} \left[C_{d,i} \frac{\pi d^2}{8} \rho_g |v_g - v_i| (v_g - v_i) - m_i g\right]$$

$$+ \frac{1}{n_i} \sum_{j=1}^{INT(i/2)} F_{j(i-j)} \left( \frac{m_j v_j + m_{i-j} v_{i-j}}{m_i} - v_i \right). \qquad (7)$$

The first term on the right-hand side of Eq. (7) is just what we would have in the absence of collisions. The second term represents the net result of all collisions; it is equal to zero if all the $v_i$ are equal because $m_j + m_{i-j} = m_i$. In reality, of course, the drops (in group i) resulting from different collisions will have different velocities. We are choosing to average over all these velocities; otherwise we would have to keep track of velocity profiles for every group of droplets, and the complexity of our numerical scheme would increase enormously.

Overall Conservation Laws. Equations (5) and (7) enable us to step along the column calculating changes in $n_i$ and $v_i$. We also need to calculate changes in $v_g$, p, and the quality x. The differentials of these three variables are computed by using the three conservation laws of mass, momentum, and energy.

Mass. The total mass flow rate is constant. Because the vapor occupies almost all of the space, we can write, to a close approximation,

$$\rho_g v_g A = w_g = xw; \qquad (8)$$

whence

$$\frac{dx}{x} = \left(\frac{d\rho_g}{dp}\right) \frac{dp}{\rho_g} - \frac{dv_g}{v_g} = \frac{dA}{A} \ . \qquad (9)$$

Mass lost by the drops appears as vapor; so

$$dw_g = -dw_f = -d \sum_{j=1}^{k} n_i m_i \ . \qquad (10)$$

We assume that evaporation occurs from all drops at a rate proportional to their mass (this seems reasonable because the latent heat is supplied by cooling the drops); therefore,

$$dm_i = \lambda m_i. \qquad (11)$$

Substituting Eq. (11) into Eq. (10) gives

$$dw_g = - \sum m_i dn_i - \lambda \sum n_i m_i \ . \qquad (12)$$

Now, $\sum m_i dn_i$ equals zero because collisions conserve mass; therefore Eq. (12) can be used to deduce the value of $\lambda$:

$$\lambda = \frac{-dw_g}{\sum n_i m_i} \ ; \qquad (13)$$

and this can be used in Eq. (11) to give

$$dm_i = \frac{-m_i}{\sum n_i m_i} dw_g \qquad (14)$$

or

$$dm_i = \frac{-m_i}{1 - x} dx \ . \qquad (15)$$

Therefore, the mass change of each droplet species can be related to changes in quality of the entire flow.

Momentum. The momentum equation for the entire flow is

$$d\left(w_g v_g + \sum_{i=1}^{k} n_i m_i v_i\right) = -Adp - A\bar{\rho}gdz \quad , \tag{16}$$

where $\bar{\rho}$ is the mean density given by

$$\bar{\rho} = \rho_g + \left(\frac{\rho_f - \rho_g}{\rho_f}\right) \sum_{i=1}^{k} \frac{n_i m_i}{A v_i} \quad . \tag{17}$$

We now wish to rearrange the left-hand side of Eq. (16) in terms of the variables to be used in the computation; thus:

$$d(w_g v_g + \sum_{i=1}^{k} n_i m_i v_i)$$

$$= v_g w dx + x w dv_g + \sum m_i v_i dn_i + \sum n_i m_i dv_i + \sum n_i v_i dm_i \quad . \tag{18}$$

We use Eq. (15) in Eq. (18) and substitute the result in Eq. (16) to get

$$\left(w v_g - \frac{\sum m_i n_i v_i}{(1-x)}\right) dx + Adp + x w dv_g$$

$$= -\bar{\rho} g A dz - \sum n_i m_i dv_i - \sum m_i v_i dn_i \quad . \tag{19}$$

The sums on the right-hand side of Eq. (19) can be derived from Eqs. (5) and (7).

Energy. The energy equation for the entire flow is

$$d\left[ wx\left(h_g + \frac{v_g^2}{2} + gz\right) + \sum_{i=1}^{k} n_i m_i \left(h_f + \frac{v_i^2}{2} + gz\right)\right] = 0. \tag{20}$$

This can be expanded as

$$w(h_g + \frac{v_g^2}{2})dx + wgdz + wx\left(\frac{dh_g}{dp}\right)dp$$

$$+ xwv_g dv_g \sum n_i m_i \left(\frac{dh_f}{dp}\right) dp + \sum n_i m_i v_i dv_i$$

$$+ \sum (n_i dm_i + m_i dn_i)\left(h_f + \frac{v_i^2}{2}\right) = 0 \quad . \tag{21}$$

Collecting terms, using Eq. (15), and realizing that $\sum m_i dn_i = 0$, we obtain

$$w\left(h_g + \frac{v_g^2}{2} - \frac{\sum n_i m_i (h_f + v_i^2/2)}{\sum n_i m_i}\right) dx$$

$$+ \left[ xw\left(\frac{dh_g}{dp}\right) + (1 - x)\, w\left(\frac{dh_f}{dp}\right)\right] dp + xwv_g dv_g$$

$$= -wgdz - \sum n_i m_i v_i dv_i - \sum m_i \frac{v_i^2}{2} dn_i \quad . \tag{22}$$

All of the thermodynamic property derivatives in Eqs. (9) and (22) are computed along the saturation line. Equations (9), (19), and (22) then form three simultaneous equations for dx, dp, and $dv_g$.

Inlet Calculations

The equilibrium pressure, temperature, and velocity of the drops and vapor at the bottom of the lift tube must be calculated to start the calculations of the mist flow. The speed of the liquid jet entering through an effective orifice area $A_o$ (including any effect of vena contracta) is

$$v_{j1} = \frac{w}{A_o \rho_f} \quad . \tag{23}$$

Using Bernouilli's equation and allowing for the pressure difference across the jet due to surface tension, we obtain for the pressure in the vapor above the injector:

$$p_1 = p_o - \frac{1}{2} \frac{w^2}{A_o^2 \rho_f} - \frac{\sigma}{r_j} \quad . \tag{24}$$

In a short length, the jet comes almost to the equilibrium temperature corresponding to $p_1$. Because the liquid makes up almost all of the mass flow and velocity changes little in this short length, momentum is conserved across the "development region" and there is little pressure change. We may therefore assume that $p_1$ exists throughout the region and the jet is cooled to the corresponding equilibrium temperature $T_1$. The mass flow of vapor is, therefore, $wC_p(T_o - T_1)/h_{fg}$. If the vapor is assumed to leave this region with uniform speed $v_{g1}$, the initial vapor velocity is

$$v_{g1} = \frac{wC_p(T_o - T_1)}{Ah_{fg}\rho_g} \tag{25}$$

because the liquid occupies only a small fraction of the volume.

| Document Control Page | 1. SERI Report No. TP-631-664 | 2. NTIS Accession No. | 3. Recipient's Accession No. |
|---|---|---|---|

4. Title and Subtitle

Analysis of the Mist Lift Process for Mist Flow Open-Cycle OTEC

5. Publication Date: June 1980

6.

7. Author(s)

Roger L. Davenport

8. Performing Organization Rept. No.

9. Performing Organization Name and Address

Solar Energy Research Institute
1617 Cole Boulevard
Golden, Colorado 80401

10. Project/Task/Work Unit No. 3451.20

11. Contract (C) or Grant (G) No.
(C)
(G)

12. Sponsoring Organization Name and Address

13. Type of Report & Period Covered: Technical Publication

14.

15. Supplementary Notes

Presented at the 1980 ASME Winter Annual Meeting; Chicago, Ill.; 16-21 Nov. 1980

16. Abstract (Limit: 200 words)

Preliminary results are presented of a numerical analysis begun by the Solar Energy Research Institute (SERI) to study the open-cycle mist flow process for ocean thermal energy conversion (OTEC). Emphasis in the analysis is on the mass transfer and fluid mechanics of the steady-state mist flow. The analysis is based on two one-dimensional models of the mist lift process: a single-group model describes a mist composed of a single size of drops and a multigroup model considers a spectrum of drop sizes. The single-group model predicts that the lift achieved in the mist lift process is sensitive to the inlet parameters. Under conditions that lead to maximum lift in the model for a single drop-size, the multigroup model predicts significantly reduced performance. Because the growth of drops is important, sensitivity of the predicted performance of the mist lift to variations in the collision parameters has been studies.

17. Document Analysis

a. Descriptors: Ocean Thermal Energy Conversion; Mist Extractors; Fluid Flow; Flow Models; Mathematical Models

b. Identifiers/Open-Ended Terms: Mist Flow Model

c. UC Categories: 64

18. Availability Statement

National Technical Information Service
U.S. Department of Commerce
5285 Port Royal Road
Springfield, Virginia 22161

19. No. of Pages: 16

20. Price: $4.00

Form No. 8200-13 (6-79)